Science Advances

AAAS

advances.sciencemag.org/cgi/content/full/2/9/e1601162/DC1

Supplementary Materials for

Evolution of anatase surface active sites probed by in situ sum-frequency phonon spectroscopy

Yue Cao, Shiyou Chen, Yadong Li, Yi Gao, Deheng Yang, Yuen Ron Shen, Wei-Tao Liu

Published 30 September 2016, *Sci. Adv.* **2**, e1601162 (2016)
DOI: 10.1126/sciadv.1601162

This PDF file includes:

S1. Basic theory of the sum-frequency generation

The basic theory for sum-frequency spectroscopy (SFS) was described elsewhere *(8-10)*. Generally, the SF signal is given by

$$S(\omega_{SF} = \omega_{vis} + \omega_{IR}) \propto \left|\chi_{eff}^{(2)}\right|^2$$

$$\chi_{eff}^{(2)} = \left[\hat{e}_{SF} \cdot \vec{L}_{SF}\right] \cdot \overleftrightarrow{\chi}_{tot}^{(2)} : \left[\hat{e}_{vis} \cdot \vec{L}_{vis}\right]\left[\hat{e}_{IR} \cdot \vec{L}_{IR}\right]$$

$$\overleftrightarrow{\chi}_{tot}^{(2)} = \overleftrightarrow{\chi}_{NR}^{(2)} + \overleftrightarrow{\chi}_{R}^{(2)}$$

where $\hat{e}_i$ and $\vec{L}_i$ are the unit polarization vector and transmission Fresnel coefficient that acts like a macroscopic local field correction factor at ω_i, and $\overleftrightarrow{\chi}_{NR}^{(2)}$ and $\overleftrightarrow{\chi}_{R}^{(2)}$ are the nonresonant background and discrete resonance contributions to the total susceptibility, $\overleftrightarrow{\chi}_{tot}^{(2)}$, of the system, respectively. $\overleftrightarrow{\chi}_{R}^{(2)}$ has the expression $\overleftrightarrow{\chi}_{R}^{(2)} = \sum_q \frac{\vec{A}_q^{(2)}}{\omega_{IR} - \omega_q + i\Gamma_q}$, with $\vec{A}_q^{(2)}$, ω_q, and Γ_q denoting the amplitude, resonant frequency, and damping of the q^{th} resonant mode of the contributing species, respectively.

S2. Calculation of the surface phonon mode of anatase (101)

The calculated phonon modes near 880 cm^{-1} are shown in fig. S1. The mode originates mainly from the stretching vibration of the Ti(5c)-O(3c) bonds with O(3c) beneath the surface. The Ti(5c)-O(3c) bonds was found to be 0.13 Å shorter than the normal Ti-O bonds in the bulk of the anatase crystal. When neighboring Ti(5c)-O(3c) bonds oscillate with the same phase (fig. S1a), the calculated resonant frequency is at 878.2 cm^{-1}, and the mode has a nonzero net dipole moment which can be detected by SFG. The dipole moment tilts by ~20^{o} from the surface normal. When neighboring Ti(5c)-O(3c) bonds oscillate with the opposite phase (fig. S1b), the mode has no net dipole moment, and the resonant frequency is at 879.9 cm^{-1}. This small frequency splitting indicates that the coupling between neighboring Ti(5c)-O(3c) bonds is weak, due to their large spatial separation.

The mode is sensitive to moieties bonded directly to Ti(5c). When there is a hydroxyl (OH) group (e. g., from water dissociation) absorbed chemically on the Ti(5c) cation, the Ti(5c)-O(3c) bond length increases significantly, and the two modes ~880 cm^{-1} disappear. Instead, new modes appear at around 701 cm^{-1} for the OH-covered (101) surface. Even greater softening will occur when heavier moieties are chemically bonded to Ti(5c), such as the O-CH_3 resulting from methanol dissociation.

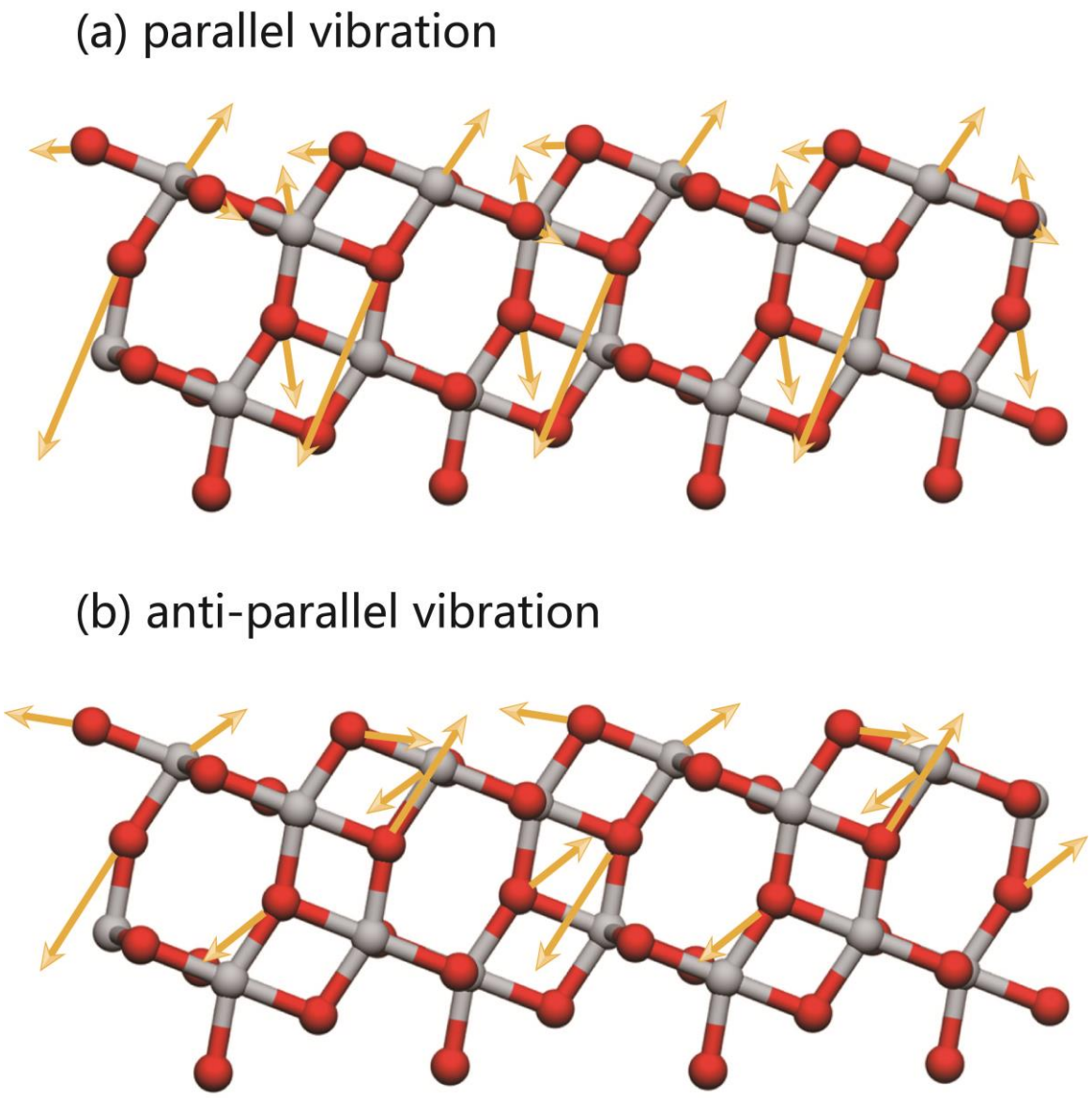

fig. S1. The calculated in-phase and out-of-phase surface phonon modes near 880 cm^{-1}. Calculated in-phase (**a**) and out-of-phase (**b**) modes ~880 cm^{-1}. The gray and red balls represent the Ti and O atoms respectively, and yellow arrows indicate the motion of ions, with the arrow length proportional to the amplitude of displacement. Ti(5c) and O(3c) ions have the greatest displacements.

S3. Symmetry properties and spectral anisotropy of the surface phonon mode on anatase (101)

The second order nonlinear susceptibility for the point group C_{1v} can be found in Ref. *37*. In the lattice coordinates, we set $a \parallel [10\bar{1}]$ (parallel to the mirror plane), $b \parallel [010]$, and $c \parallel [101]$. We have $\chi^{(2)}_{R,lmn} \propto R_{lm}\mu_n$ $(l,m,n \in \{a,b,c\})$, with R_{lm} and μ_n denoting the Raman tensor element and infrared dipole derivative moment of the localized phonon mode, respectively. With this convention, phonon modes belonging to the A' irreducible representation have the following nonzero $\overleftrightarrow{\chi}^{(2)}$ elements, (with $\chi^{(2)}_{abc}$ written as abc) $aaa, aac, aca, acc, bba, bbc, caa \approx aca, cac \approx acc, cca,$ and ccc, where "≈" holds due to negligible dispersion in the response of anatase to SF and near-IR fields. For modes of the $A"$ irreducible representation, the nonvanishing elements of $\overleftrightarrow{\chi}^{(2)}$ are $abb, bab, bcb,$ and ccb.

The $\overleftrightarrow{\chi}^{(2)}$ elements expressed in the lab coordinates (x,y,z) are related to those in the crystal coordinates (a,b,c) by $\chi^{(2)}_{ijk} = \sum_{lmn} \chi^{(2)}_{lmn}(\hat{\imath}\cdot\hat{l})(\hat{\jmath}\cdot\hat{m})(\hat{k}\cdot\hat{n})$, with $i,j,k \in \{x,y,z\}$ and $l,m,n \in \{a,b,c\}$. In our SFG measurements, the lab coordinates (x,y,z) are defined with z along the sample surface normal (as well as the c-axis), and y perpendicular to the incident plane. When a is at angle ϕ from the beam incident plane, we have $\hat{a} = \cos\phi\hat{x} + \sin\phi\hat{y}$, $\hat{b} = -\sin\phi\hat{x} + \cos\phi\hat{y}$ and $\hat{c} = \hat{z}$. Expressions of the $\overleftrightarrow{\chi}^{(2)}$ elements in the lab for different ϕ angles can then be found.

In the measurement, the incident and outgoing angles for the NIR and SF beams are both near $45°$, and we have $\overleftrightarrow{L}(\omega_{SF}) \approx \overleftrightarrow{L}(\omega_{NIR})$. Therefore, when the incident plane is parallel to the surface mirror plane ($\phi = 0$ and $180°$), we have, for the A' mode, $\chi_{\parallel}^{(2)}(SPS)\big|_{A'} = \chi_{\parallel}^{(2)}(PSS)\big|_{A'} = 0$, and $\chi_{\parallel}^{(2)}(SSP)\big|_{A'}$, $\chi_{\parallel}^{(2)}(PPP)\big|_{A'}$ are both proportional to $[\pm\mu_a \cdot \cos\beta_{IR} L_{xx}^{\parallel}(\omega_{IR}) + \mu_c \cdot \sin\beta_{IR} L_{zz}^{\parallel}(\omega_{IR})]$. The plus (minus) sign in "$\pm$" holds for $\phi = 0$ ($180°$). For the $A"$ mode, we have $\chi_{\parallel}^{(2)}(SSP)\big|_{A"} = \chi_{\parallel}^{(2)}(PPP)\big|_{A"} = 0$, and $\chi_{\parallel}^{(2)}(SPS)\big|_{A"}$, $\chi_{\parallel}^{(2)}(PSS)\big|_{A"}$, are both $\propto \mu_b \cdot L_{yy}^{\parallel}(\omega_{IR})$. Hence, for $\phi = 0$ and $180°$, the $A"$ mode should show up only in SPS and PSS spectra, and the A' mode only in SSP and PPP spectra. This allows us to distinguish A' and $A"$ modes unambiguously.

In terms of azimuthal anisotropy, the above analysis shows that the A' mode should have its amplitude vary with ϕ from 0 to $180°$ in both SSP and PPP spectra. At $\phi = 90°$ and $270°$, the incident plane is perpendicular to the mirror plane at the surface, and we have both $\chi_{\perp}^{(2)}(SSP)\big|_{A'}$ and $\chi_{\perp}^{(2)}(PPP)\big|_{A'} \propto \mu_c \cdot \sin\beta_{IR} L_{zz}^{\perp}(\omega_{IR})$. The A' mode therefore should have the same amplitude at $\phi = 90°$ and $270°$. The 860 cm^{-1} we observed in our experiment has all the above symmetry properties of the A' mode.

As shown above, the intensity ratio of the A' mode for both SSP and PPP polarization combinations is given by $S_{SF}(\phi = 180°)/S_{SF}(\phi = 0°) \approx \left|(\mu_{a,eff} - \mu_{c,eff})/(\mu_{a,eff} + \mu_{c,eff})\right|^2$, with $\mu_{a,eff} = \mu_a \cdot \cos\beta_{IR} L_{xx}^{\parallel}(\omega_{IR})$ and $\mu_{c,eff} = \mu_c \cdot \sin\beta_{IR} L_{zz}^{\parallel}(\omega_{IR})$ being effective transition dipole moments along the a and

$c$axes, respectively. Experimentally, we found $S_{SF}(\phi = 180°)/S_{SF}(\phi = 0°) \approx 0.012 \pm 0.001$, hence $|\mu_{a,eff}/\mu_{c,eff}| \approx 1.0 \pm 0.2$, from which we deduce $|\mu_a/\mu_c| \approx 0.47 \pm 0.02$. For the bond tilting angle, θ, from the c axis, there is $\tan\theta = \frac{\mu_a}{\mu_c}$, which yields $\theta \approx 25 \pm 5°$.

S4. Adsorbed methanol on anatase (101)

Spectra in the C-H stretching vibration range of anatase (101) in saturated methanol vapor are presented in fig. S2. The two major resonant modes at ~ 2840 and 2955 cm^{-1} are symmetric and anti-symmetric stretching vibration, respectively, of the CH_3 group of molecular methanol. Corresponding modes of the CH_3 group of methoxy, if present due to methanol dissociation, are expected to appear at ~ 2828 and 2935 cm^{-1}*(38)*, but were not observed within our detection limit. Upon uv irradiation, the non-resonant background signal increases slightly as also seen for methanol/rutile (110) *(29)*, and methoxy signal was still not observable.

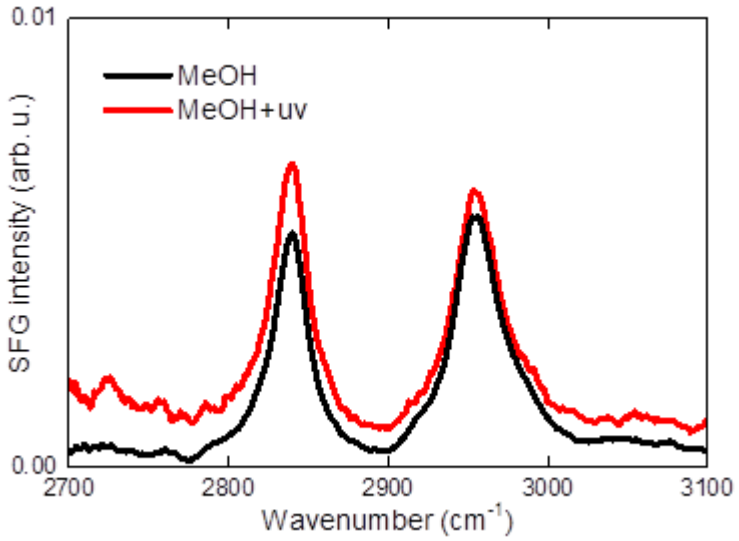

fig. S2. SFG spectra in the C–H stretching vibration range for adsorbed methanol on anatase (101).

S5. Calculation on the stability of oxygen vacancies on anatase (101) exposed to ambient gases

The optimized adsorption configuration calculated for methanol, water, N_2 and H_2 molecules are presented in fig. S3. Table S1 shows the calculated energy difference between oxygen vacancies at the surface and in the sub-surface of anatase (101), [$\Delta E = E(V_O^{surf}) - E(V_O^{sub})$], affected by various molecules in the ambient gas.

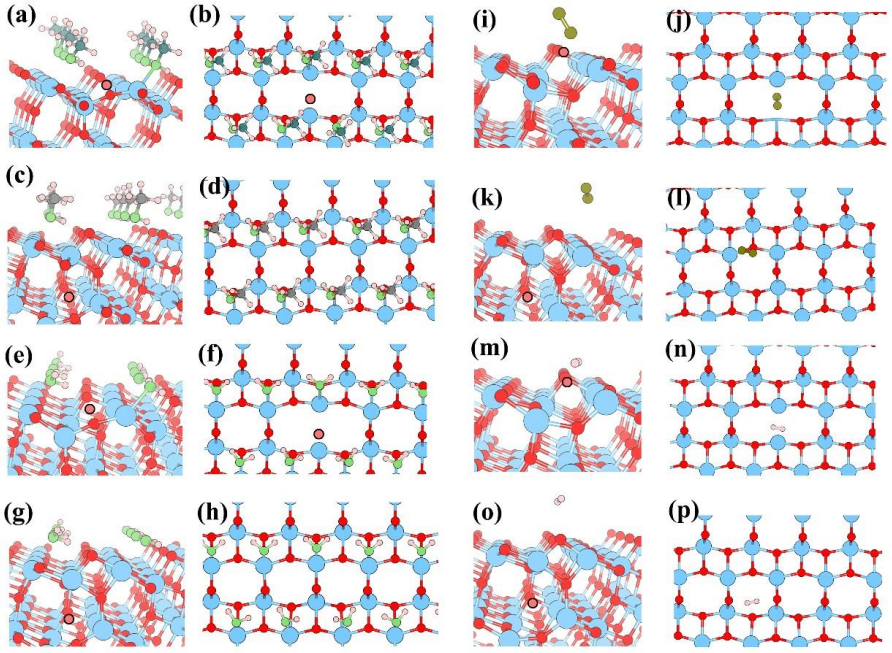

fig. S3. Optimized surface structures of anatase (101) with various ambient molecules. Top and side views of optimized surface structures of anatase (101) with monolayers of methanol (**a-d**) and water (**e-h**), N_2 (**i-l**) and H_2 (**m-p**) on it. Ti and O from TiO_2, and O, C, H, and N from adsorbed molecules are denoted by light blue, red, light green, dark green, pink and olive green balls, respectively. The oxygen vacancy (Vo) sites are represented by black circles filled with red.

table S1. Energy difference between V_O^{surf} and V_O^{sub} of anatase (101) in different ambient environment.

Environment	ΔE (eV)
Clean surface in vacuum	0.46
H_2 monomer	0.30
N_2 monomer	0.21
Water monolayer	0.16
Methanol monolayer	0.09

S6. The removal of hydrocarbon contaminants by UV-ozone treatment

The hydrocarbon contaminants on anatase surface can be effectively removed by the uv-ozone treatment. fig. S4 shows SFG spectra of the anatase sample before (blue) and after (red) uv-onzone treatment in the C-H stretching vibration frequency range. The resonant peaks at ~2850, 2880 and 2950 cm^{-1} are due to surface hydrocarbon contaminants.

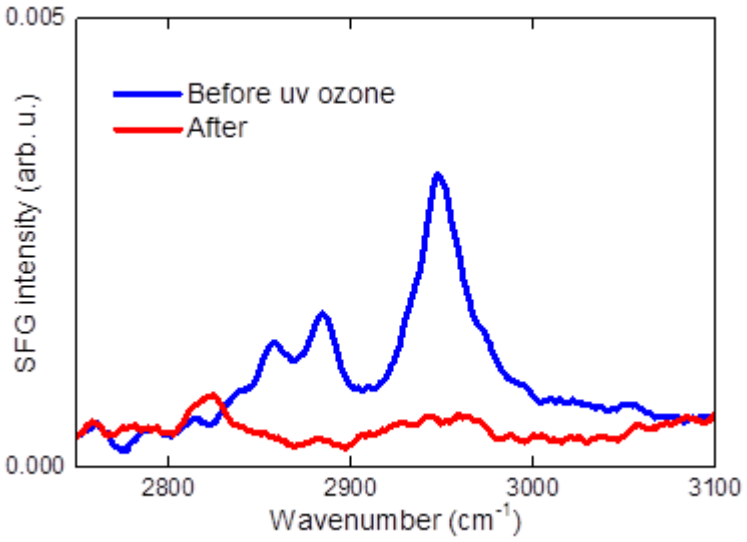

fig. S4. SFG spectra of anatase (101) in the C–H stretching vibration range for hydrocarbon contaminants before and after UV-ozone treatment.